ACS Macro Letters

Letter

Cite This: ACS Macro Lett. 2019, 8, 155−160

pubs.acs.org/macroletters

Threading of Unconcatenated Ring Polymers at High Concentrations: Double-Folded vs Time-Equilibrated Structures

Jan Smrek,*[,†,‡] Kurt Kremer,*[,†] and Angelo Rosa*[,§]

[†]Max Planck Institut for Polymer Research, Ackermannweg 10, D-55128 Mainz, Germany

[‡]Faculty of Physics, University of Vienna, Boltzmanngasse 5, A-1090 Vienna, Austria

[§]SISSA (Scuola Internazionale Superiore di Studi Avanzati), Via Bonomea 265, 34136 Trieste, Italy

Supporting Information

ABSTRACT: Unconcatenated ring polymers in concentrated solutions and melt are remarkably well described as double-folded conformations on randomly branched primitive trees. This picture though contrasts recent evidence for extensive intermingling between close-by rings in the form of long-lived topological constraints or threadings. Here, we employ the concept of ring minimal surface to quantify the extent of threadings in polymer solutions of the double-folded rings vs rings in equilibrated molecular dynamics computer simulations. Our results show that the double-folded ring polymers are significantly less threaded compared to their counterparts at equilibrium. Second, threadings form through a slow process whose characteristic time-scale is of the same order of magnitude as that of the diffusion of the rings in solution. These findings are robust, being based on universal (model-independent) observables as the average fraction of threaded length or the total penetrations between close-by rings and the corresponding distribution functions.

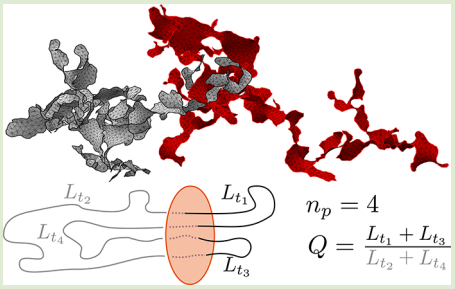

Concentrated solutions and melts of unconcatenated and unknotted ring polymers have stimulated intensive theoretical[1−20] and experimental[21−27] work in the past years.

Under high concentrations rings challenge most of the peculiarities characterizing the more familiar case of solutions of *linear* chains. First, spatial constraints arising from global topological invariance and the consequential departure[4] from the Flory-like mechanism[28−30] for compensation of excluded volume effects imply that the average ring size or gyration radius, R_g, scales in the limit of large polymer mass or contour length, L_c, like[11,12] $R_g \sim L_c^{1/3}$, while for linear chains[28−30] $R_g \sim L_c^{1/2}$. Second, the absence of free ends implies that rings do not relax via common reptation which is, instead, the dominating mechanism for linear chains.[28−30] Consequently, stress relaxation in ring solutions decays as a power-law[21] with no sign of the rubber-like plateau of linear melts.[29,30]

Substantial theoretical progress was made back in the '80s, when Khokhlov and Nechaev[1] and Rubinstein[31] mapped the problem of rings in entangled solutions to the one of a single ring in an array of fixed obstacles to which it is not topologically linked. In the latter conditions, rings should adopt double-folded conformations on randomly branching primitive trees.[1,31] Recently,[11] explicit numerical mapping of ring polymers in solution to randomly branched structures has demonstrated that relevant properties such as the polymer gyration radius or contact frequencies can be accurately reproduced. Further theoretical and numerical investigations[12,15,18,32] also support the "rings/branched polymers" analogy.

This successful picture is challenged in recent works[33] showing that mutually exposed surfaces between neighbor rings form long-lived topological constraints, commonly known as *threadings*.[17,20,34,35] Absent in systems of linear chains, threadings are responsible for the observed glassy behavior of ring solutions under pinning perturbations.[17,20,36] Conversely, being relaxed only up to the entanglement scale (Section IA in SI), ring polymers folding into branched structures display little interpenetration with close-by neighbors.

To shed light on this apparent conflict, in this Letter we quantify the extent of threadings between distinct pairs of unconcatenated rings in solution and melt by employing the concept of ring *minimal surface* (Figure 1(A), top), which was recently[10,33] applied to detect threadings in melts of rings. Specifically, a ring is defined as "threaded" by another ring if its minimal surface is crossed by the other ring (Figure 1(A), bottom). Here we investigate only two-ring threadings; therefore, self-threadings are ignored. Numerical construction of minimal surfaces has been performed in turn for: (1) double-folded ring polymers on interacting randomly branched primitive trees[11] (IBP model) (for details, see Sec. IA in Supporting Information (SI)) and (2) rings in solutions equilibrated through large-scale, brute-force molecular dynamics (MD) computer simulations. As for the latter, two microscopic, distinct polymer models have been chosen (Sec.

Received: October 28, 2018
Accepted: December 12, 2018

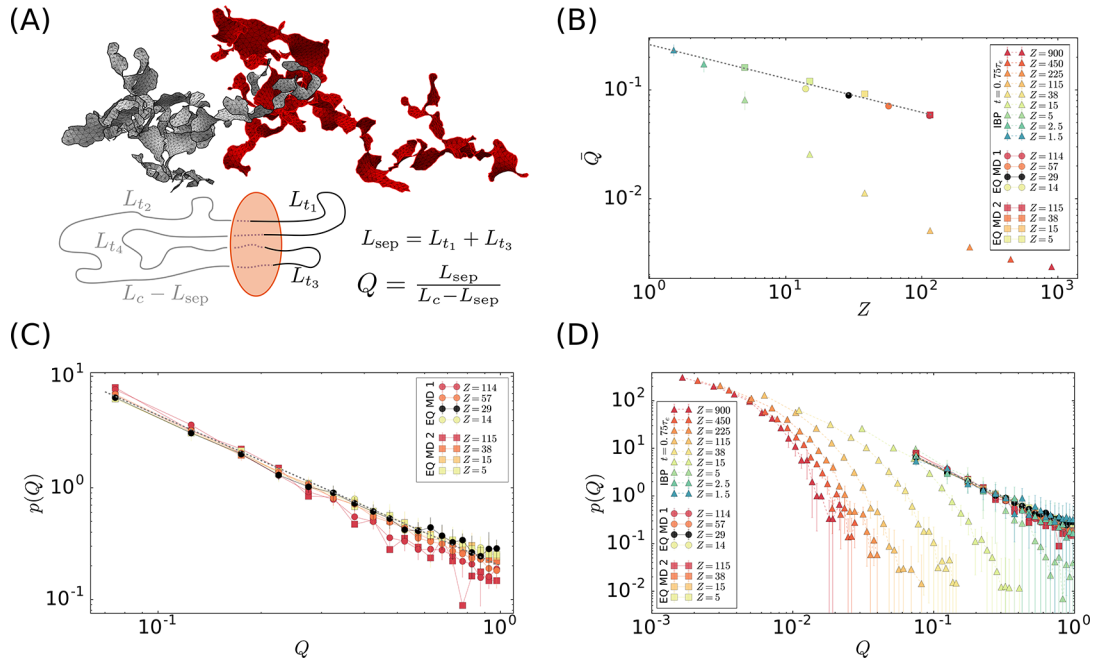

Figure 1. Threading statistics in terms of relative contour length fraction Q. (A) Top: Minimal surfaces of a pair of close-by rings modeled as double-folded polymers on interacting branched primitive trees (IBP model). Bottom: Schematic representation of one ring (black and gray) penetrating the minimal surface of another ring (orange) of total contour length L_c. L_{t_i} is the contour length of subchain i penetrating the second ring. In this example, four surface penetrations ($n_p = 4$) split the penetrating ring into the segment pairs (L_{t_1},L_{t_3}) and (L_{t_2},L_{t_4}) which are on opposite sides of the surface: this defines the separation length, L_{sep}, and its complementary, $L_c - L_{sep}$. Adapted with permission from ref 33. (B) Mean relative contour length fraction, $\bar{Q}$, of one ring threading another ring as a function of ring mass, Z. The dashed line is the best fit to the data for MD-equilibrated rings, $\bar{Q} \approx 0.26Z^{-0.31}$. (C) Probability distribution functions, $p(Q)$ (log−log scale). Results for MD-equilibrated rings from polymer models EQ MD 1 and EQ MD 2. The dashed gray line $p(Q) \sim Q^{-1.35}$ is the best fit to the distributions tail. (D) Comparison between $p(Q)$'s for the IBP model and MD-equilibrated rings. In panels (C) and (D), the bin size is $Q_{max}/20$ with Q_{max} being the largest value of Q in the given data set.

IB in SI): (a) the classical Kremer−Grest (KG) polymer model (hereafter, EQ MD 1) from ref 7 at melt conditions and (b) the generalized KG polymer model (hereafter, EQ MD 2) from refs 11 and 37 with larger stiffness at semidilute conditions. The initial ring conformations adopted in this second case come from the IBP model, and thus we will use the full MD trajectories to characterize the time progression of the threading statistics. To analyze results from the two different polymer models on equal footing, observables will be given as functions of the total number of entanglements $Z \equiv L_c/L_e$,[38,39] where L_c is the ring contour length and L_e is the entanglement length.[29] The largest rings which can be equilibrated in reasonable computational time are for $Z \approx 100$ for both setups (see Table S1 in SI for details on the systems and corresponding statistics used). To speed up the equilibration of the longest rings of EQ MD 1, we used a novel anisotropic doubling scheme (see Sec. IB in SI).

Threadings statistics: Minimal surfaces spanned on the ring polymers are obtained by a slightly modified version of the minimization algorithm from ref 33 (see Sec. IC in SI). The algorithm is based on successive iterations of triangulations evolving under surface tension by moving the free vertices. Typically, each ring penetrates the minimal surfaces of more of its neighbors, and this number grows with Z (see Sec. IE in SI for details). Then, following ref 33 we introduce the *separation length*

$$L_{sep} = \min\left(\sum_{i=\text{even}} L_{t_i}, \sum_{i=\text{odd}} L_{t_i}\right) \quad (1)$$

where L_{t_i} is the (threading) length between the i-th and the (i + 1)-th penetrations of the surface (Figure 1(A), bottom). L_{sep} characterizes how much material of the *penetrating* ring is on one side of the *penetrated* ring (the contour length on the other side being $L_c - L_{sep}$, of course). Accordingly, the quantity $Q \equiv \frac{L_{sep}}{L_c - L_{sep}}$ accounts for the relative extent of contour length on one side with respect to the other, $Q = 1$, meaning the penetrating ring is half split by the penetrated surface.

The mean value $\bar{Q} = \bar{Q}(Z)$, obtained by averaging Q over $O(10^3)$ up to $O(10^4)$ interpenetrating rings pairs (see Table S1 in SI), is plotted in Figure 1(B). Remarkably, data for MD-equilibrated rings collapse on the same (universal) curve characterized by simple power-law decay $\bar{Q} = (0.26 \pm 0.09)$ $Z^{-0.31\pm0.09}$ (dashed line). As the two polymer models EQ MD 1 and 2 have different monomer densities and entanglement lengths (Sec. IB in SI), this is a nontrivial result, which pinpoints $\bar{Q}$ as a suitable "order parameter" for characterizing the total extent of threading between close-by rings. In fact, double-folded rings display smaller values for $\bar{Q}$ suggesting a lesser extent of threadings between close-by rings. Figure 1(C) shows the complete distribution functions, $p(Q)$, for MD-equilibrated rings at different Z's. Mirroring corresponding averages in Figure 1(B), $p(Q)$'s from the two different polymer models agree well, and the observed power-law behavior $p(Q)$

DOI: 10.1021/acsmacrolett.8b00828
ACS Macro Lett. 2019, 8, 155−160

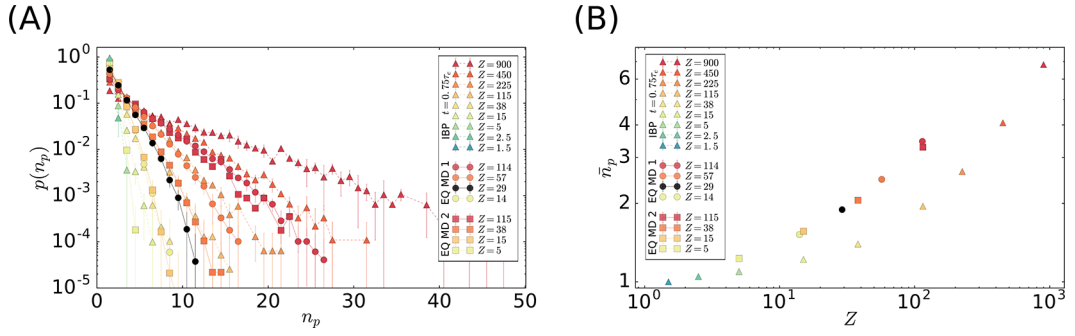

Figure 2. Threading statistics in terms of number of penetrations. (A) Probability distribution functions, $p(n_p)$, of the number of penetrations, n_p, for the different polymer models and ring masses Z (linear-log scale). (B) Corresponding mean number of penetrations, $\bar{n}_p$, as a function of the ring mass, Z (log–log scale).

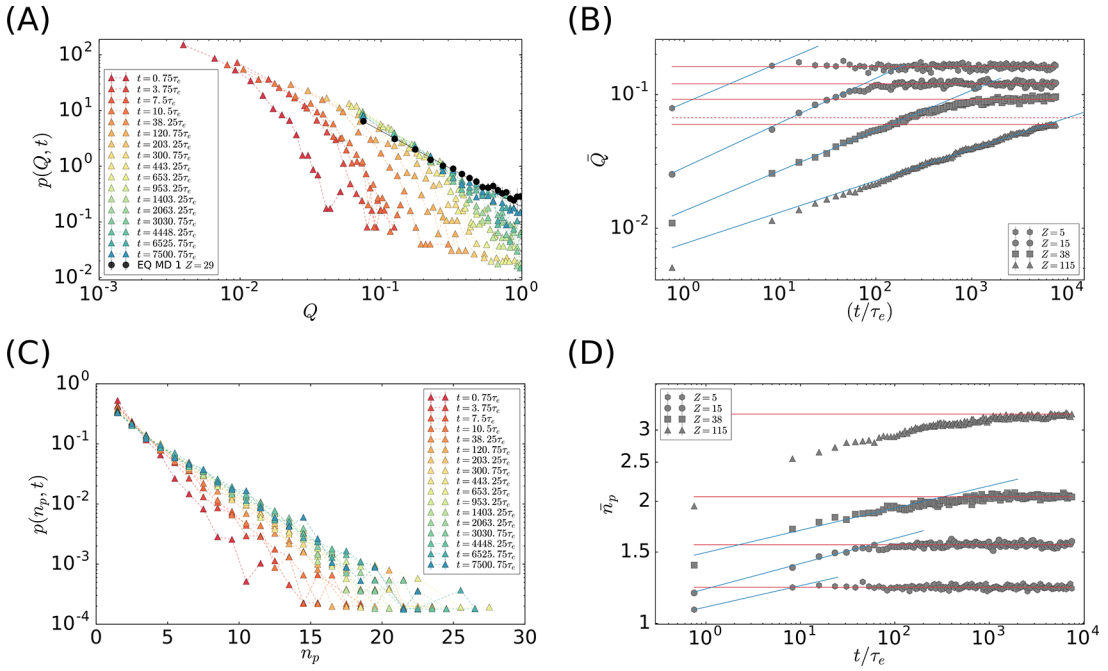

Figure 3. Time evolution of threading statistics. (A) Time-dependent distribution functions, $p(Q,t)$, of the relative contour length fraction, Q, of one ring threading another ring (log–log scale). Results for solutions of rings with $Z = 115$ prepared according to the IBP model. Similar curves are found also for other Z's (not shown). Black circles represent the equilibrium distribution $p(Q)$ calculated for rings with $Z = 29$ (Figure 1(C)). (B) Corresponding mean values, $\bar{Q}(t)$ (symbols), as functions of time (log–log scale) and power-law fits to the data (eq 2, blue lines) in the initial stage of the equilibration. Solid horizontal lines for $Z = 5$, 15, and 38 denote corresponding equilibrium values $\bar{Q}(Z)$. For $Z = 115$, the solid line is for the value measured at the end of the trajectory, and the dashed line is for the extrapolated equilibrium value. (C) Time-dependent distribution functions, $p(n_p,t)$, of the number of penetrations, n_p (linear-log scale). Similar curves are found also for other Z's (not shown). (D) Corresponding mean number of penetrations, $\bar{n}_p(t)$ (symbols), as functions of time (log–log scale) and power-law fits to the data (eq 3, blue lines) in the initial stage of the equilibration. Horizontal lines are for asymptotic values $\bar{n}_p(Z)$.

$\sim Q^{-1.35}$ for $0.1 \lesssim Q \lesssim 1$ agrees with the reported[33] decay for distribution functions, $p(L_{sep})$, of separation length. In turn, expecting that the minimal size of penetrating length is $O(L_e)$, the average value $\bar{Q} \approx \int_{1/Z}^{1} Q^{-0.35}\, dQ / \int_{1/Z}^{1} Q^{-1.35}\, dQ \approx 0.54\, Z^{-0.35}$ is consistent with the power-law behavior reported in Figure 1(B). Small, systematic differences toward $Q \to 1$ between $p(Q)$'s for rings with $Z = 114$ and $Z = 115$ should be attributed to incomplete equilibration of the corresponding data sets (see discussion in Sec. IB in SI). As explained in the following, such deviations from the equilibrium distribution emerge also for smaller Z's whenever polymer chains are not fully equilibrated. In sharp contrast with the results for equilibrated rings, $p(Q)$ distributions for rings constructed according to the IBP model decay very differently (Figure 1(D)). This is particularly evident for very large rings, whose $p(Q)$'s feature an exponential cutoff toward $Q \to 1$. As the fine structure of the IBP rings is, by construction, relaxed only up to spatial scales of the order of $Z \approx 1$ (Sec. IA in SI), we suspect threadings between large rings have not yet relaxed. Consistent with that, very short IBP rings ($Z = 1.5$) are instead fully relaxed, as the corresponding $p(Q)$ exhibits the same universal equilibrium form from Figure 1(C).

We complete the discussion by focusing on how many times (n_p) any ring penetrates the minimal surface of any other single ring. In order to dismiss any fine scale detail related to the employed polymer model, a given threading segment contributes to n_p only if its contour length exceeds the entanglement length L_e.[38] We notice, though, that with this constraint n_p is not necessarily an even number as in the

DOI: 10.1021/acsmacrolett.8b00828
ACS Macro Lett. 2019, 8, 155–160

original work.[33] Figure 2(A) shows that distribution functions $p(n_p)$'s display exponential tails for both MD-equilibrated rings (in agreement with ref 33) and IBP-model rings. Instead, corresponding *mean* values $\overline{n}_p \equiv \int n_p p(n_p) dn_p$ as functions of ring mass Z behave differently for MD-equilibrated vs IBP rings (Figure 2(B)). As for $\overline{Q}(Z)$, $\overline{n}_p(Z)$ from different MD simulations nicely collapses on a single curve. However, at odds with $\overline{Q}(Z)$ (Figure 1(B)), $\overline{n}_p(Z)$ is laying at the threshold of a (slow) crossover, and consequently, our attempt to fit the data for $Z \geq 29$ to a single power-law behavior gave poor results. Obviously, the lower values for $\overline{n}_p(Z)$ from non-equilibrated rings reflect, as for $\overline{Q}(Z)$, how these chains systematically "underthread" their spatially close neighbors. Due to the exponential character of the $p(n_p)$ distributions and the fact that each ring threads its neighbors (see Sec. IE in SI), the mean value $\overline{n}_p$ is a good indicator of the typical number of penetrations made by a single ring.

Threadings dynamics: We are now going to discuss how almost unthreaded rings constructed according to the IBP model progressively thread each other. These rings reproduce several properties of equilibrated ring conformations like the gyration radius and contact probabilities.[11] On the other hand (Figures 1 and 2), they fail in reproducing threading statistics. Therefore, we track how threading statistics is changing as ring conformations are relaxing over time. In the following, time is always expressed in units of the entanglement time τ_e,[29] corresponding to the characteristic time scale above which entanglements start slowing down chain dynamics.

Figure 3(A) shows the evolution of the distribution function $p(Q,t)$ for $Z = 115$ (similar plots are obtained for $Z = 5$, 15, and 38, not shown) at different times. For short times, the distribution $p(Q,t)$ is a power-law for $Q \to 0$ and has an exponential cutoff at larger $Q \to 1$, as in Figure 1(D). As time increases, the exponential cutoff is progressively shifting to larger Q values as longer threadings occur. Then, we consider how the mean value, $\overline{Q}(t) \equiv \int Q p(Q,t) dQ$, changes with time (Figure 3(B)). Interestingly, $\overline{Q}(t)$ grows at early times according to the simple power-law:

$$\overline{Q}(t) \sim (t/\tau_e)^{\alpha_Q} \tag{2}$$

For $Z = 5$, 15, and 38 this regime is followed by a plateau, implying that equilibrium has been reached. Best fits of eq 2 to the data before the plateau (blue lines in Figure 3(B)) give effective exponents $\alpha_Q \approx 0.3$ (for specific values, see Table S2 in SI). The heights of the different plateaus correspond (solid horizontal lines) to the equilibrium values for $\overline{Q}(Z)$ (symbols "□" in Figure 1(B)). For $Z = 115$ instead, due to the incomplete equilibration, threadings are still evolving. In this case, the height of the corresponding plateau (dashed horizontal line) is *extrapolated* from the reported (Figure 1(B)) power-law behavior $\overline{Q}(Z) \approx 0.26 Z^{-0.31}$. The intercept between the fitted power-law and the plateau defines the threading relaxation time, $\tau^{th}_{rel,Q}(Z)$ (for specific values, see Table S2 in SI). Interestingly, $\tau^{th}_{rel,Q}(Z)$ is of the same order of the relaxation times, $\tau^{diff}_{rel}(Z)$, associated with ring thermal diffusion (Table S2 in SI) and defined (see Sec. IB in SI) at the intercept between the time mean-square displacement of the ring center of mass, $\langle g_3(t) \rangle \equiv \langle (\vec{r}_{cm}(t) - \vec{r}_{cm}(0))^2 \rangle$, and the time-dependent mean-square gyration radius, $\langle R_g^2(t) \rangle$. On the other hand, τ^{diff}_{rel} is expected[8] to be significantly larger than the time scale associated with *internal* ring motion,[8] $\tau^{int}_{rel} \equiv \int_0^\infty \frac{\langle \vec{c}(t) \cdot \vec{c}(0) \rangle}{\langle c(0)^2 \rangle} dt$, where $\vec{c}(t) = \vec{d}_1(t) \times \vec{d}_2(t)$ and $\vec{d}_1(t)$ and $\vec{d}_2(t)$ are any arbitrarily chosen pair of spanning ring diameters whose tails are separated by the contour length $Z/4$. Accurate numerical evaluation of τ^{int}_{rel} (see Sec. IB in SI) confirms that $\tau^{int}_{rel} < \tau^{diff}_{rel}$ at any given Z (Table S2 in SI). Threadings constitute then the dominant degrees of freedom governing ring relaxation.

We complete our analysis by considering the time evolution of the distribution function of the number of penetrations, $p(n_p,t)$, as the rings progressively thread (Figure 3(C)) as well as the corresponding average value, $\overline{n}_p(t) \equiv \int n_p p(n_p,t) dn_p$ (Figure 3(D)). Data appear slightly noisier than the ones for $\overline{Q}(t)$ (Figure 3(B)), yet $\overline{n}_p(t)$ is also clearly exhibiting an initial power-law regime

$$\overline{n}_p(t) \sim (t/\tau_e)^{\alpha_{n_p}} \tag{3}$$

followed by given plateaus for $Z = 5$, 15, and 38 whose heights (solid horizontal lines) correspond to the equilibrium values $\overline{n}_p(Z)$ (symbols "□" in Figure 2(B)). In those cases, the effective exponents α_{n_p} are close to ≈0.06, while the crossover times $\tau^{th}_{rel,n_p}(Z)$ match well the corresponding $\tau^{th}_{rel,Q}(Z)$'s (Table S2 in SI). As for $Z = 115$, arguably because of incomplete equilibration, the initial crossover to equilibrium resembles less a single power-law compared to the other cases with smaller Z. Since the evaluation of the asymptotic behavior at large t is also problematic (see discussion on threading statistics), corresponding α_{n_p} and τ^{th}_{rel,n_p} cannot be reliably estimated.

Conclusions: Theoretical considerations[1,3,31] corroborated by recent numerical work[11] led to the conclusion that topologically constrained ring polymers like rings in a gel[36] or rings in concentrated solutions and melt[7,8,11,12] should resemble double-folded conformations with randomly branched structures.

In this Letter, we have shown that this picture is not complete as it tends to underestimate the correct extent of threadings[17,20,34,35] between close-by rings at equilibrium. Following refs 10 and 33 our analysis relies upon the concept of ring minimal surface, and our results are independent from model details: in particular we report that both the relative contour length penetrating the minimal surface of a given ring (Q and its distribution $p(Q)$, Figure 1) and the absolute number of penetrations (n_p and its distribution $p(n_p)$, Figure 2) display universal features. At the same time, we have demonstrated that threading relaxation to equilibrium (functions $\overline{Q}(t)$ and $\overline{n}_p(t)$, Figure 3) is power-law and that the associated time scales match ring diffusion in melt while remaining significantly larger than the time scales associated with ring internal relaxation. Based on that, we predict that threadings dominate ring relaxation in entangled solutions. At the same time, two of our results also hint on the reason why double-folded models work well:[11] (1) the observed relation $\overline{Q}(Z)^{-1} = (Z - Z_{sep})/Z_{sep} \sim Z^{0.31}$ implying that the separation length $Z_{sep} \equiv L_{sep}/L_e$ increases only sublinearly in the ring mass Z and (2) the small (Figure 2(B)) mean number of threadings. The static properties could then be well governed by the larger unthreaded contour length $L_c - L_{sep}$, in agreement with the tree picture. Yet, the smaller L_{sep} could affect the dynamics.

We speculate that the exponent $\alpha_Q \approx 0.3$ governing threading relaxation could be (related to) the exponent 1/3 of the late-stage phase-ordering kinetics with a conserved order parameter.[40−42] If the number of branches of the ring conformation is conserved during the relaxation from the IBP state, the curvilinear diffusion of the branches could be

DOI: 10.1021/acsmacrolett.8b00828
ACS Macro Lett. 2019, 8, 155−160

viewed as switching the branches from a nonthreading to a threading state. To find out if the correspondence does exist, we would need to connect our threading analysis with an algorithm to detect branches such as the one in ref 18.

A limitation of the present analysis is that while concentrating primarily on pairwise threadings it neglects higher-order ones whose contribution to ring dynamics in melts appears to be not negligible.[35] In the future, a potential noninvasive method to detect the complex threadings could help to clarify their microscopic origin and effect.

In light of these results, the question related to how to construct "by first-principles" equilibrated solutions of ring polymers not based on double-folded conformations[11] is still open: whether the answer will require us to rethink double-folded conformations or a completely different approach, in both cases it remains a promising research line for the future.

■ ASSOCIATED CONTENT

Supporting Information

The Supporting Information is available free of charge on the ACS Publications website at DOI: 10.1021/acsmacrolett.8b00828.

Additional details on: preparation of initial melts of ring conformations, molecular dynamics computer simulations, and the algorithm to compute minimal surfaces (PDF)

■ AUTHOR INFORMATION

Corresponding Authors

*E-mail: jan.smrek@univie.ac.at.
*E-mail: kremer@mpip-mainz.mpg.de.
*E-mail: anrosa@sissa.it.

ORCID

Jan Smrek: 0000-0003-1764-9298
Kurt Kremer: 0000-0003-1842-9369

Notes

The authors declare no competing financial interest.

■ ACKNOWLEDGMENTS

We thank Alexander Grosberg and Michael Lang for useful discussions. J.S. acknowledges support from the Austrian Science Fund (FWF) through the Lise-Meitner Fellowship No. M 2470-N28. The authors would like to acknowledge networking support by the COST Action CA17139. This work has been supported by the European Research Council under the European Union's Seventh Framework Programme (FP7/2007-2013)/ERC Grant Agreement No. 340906-MOL-PROCOMP. We are grateful to the Max Planck Computing and Data Facility (MPCDF).

■ REFERENCES

(1) Khokhlov, A. R.; Nechaev, S. K. Polymer chain in an array of obstacles. *Phys. Lett. A* **1985**, *112A*, 156−160.
(2) Grosberg, A. Y.; Nechaev, S. K.; Shakhnovich, E. I. The role of topological constraints in the kinetics of collapse of macromolecules. *J. Phys. (Paris)* **1988**, *49*, 2095−2100.
(3) Obukhov, S. P.; Rubinstein, M.; Duke, T. Dynamics of a ring polymer in a gel. *Phys. Rev. Lett.* **1994**, *73*, 1263−1266.
(4) Müller, M.; Wittmer, J. P.; Cates, M. E. Topological effects in ring polymers: A computer simulation study. *Phys. Rev. E: Stat. Phys., Plasmas, Fluids, Relat. Interdiscip. Top.* **1996**, *53*, 5063−5074.
(5) Müller, M.; Wittmer, J. P.; Cates, M. E. Topological effects in ring polymers. II. Influence of persistence length. *Phys. Rev. E: Stat. Phys., Plasmas, Fluids, Relat. Interdiscip. Top.* **2000**, *61*, 4078−4089.
(6) Suzuki, J.; Takano, A.; Deguchi, T.; Matsushita, Y. Dimension of ring polymers in bulk studied by Monte-Carlo simulation and self-consistent theory. *J. Chem. Phys.* **2009**, *131*, 144902.
(7) Halverson, J. D.; Lee, W. B.; Grest, G. S.; Grosberg, A. Y.; Kremer, K. Molecular dynamics simulation study of nonconcatenated ring polymers in a melt. I. Statics. *J. Chem. Phys.* **2011**, *134*, 204904.
(8) Halverson, J. D.; Lee, W. B.; Grest, G. S.; Grosberg, A. Y.; Kremer, K. Molecular dynamics simulation study of nonconcatenated ring polymers in a melt. II. Dynamics. *J. Chem. Phys.* **2011**, *134*, 204905.
(9) Sakaue, T. Ring Polymers in Melts and Solutions: Scaling and Crossover. *Phys. Rev. Lett.* **2011**, *106*, 167802.
(10) Lang, M. Ring Conformations in Bidisperse Blends of Ring Polymers. *Macromolecules* **2013**, *46*, 1158−1166.
(11) Rosa, A.; Everaers, R. Ring polymers in the melt state: the physics of crumpling. *Phys. Rev. Lett.* **2014**, *112*, 118302.
(12) Grosberg, A. Y. Annealed lattice animal model and Flory theory for the melt of non-concatenated rings: towards the physics of crumpling. *Soft Matter* **2014**, *10*, 560−565.
(13) Narros, A.; Likos, C. N.; Moreno, A. J.; Capone, B. Multi-blob coarse graining for ring polymer solutions. *Soft Matter* **2014**, *10*, 9601−9614.
(14) Michieletto, D.; Marenduzzo, D.; Orlandini, E.; Alexander, G. P.; Turner, M. S. Threading Dynamics of Ring Polymers in a Gel. *ACS Macro Lett.* **2014**, *3*, 255−259.
(15) Smrek, J.; Grosberg, A. Y. Understanding the dynamics of rings in the melt in terms of the annealed tree model. *J. Phys.: Condens. Matter* **2015**, *27*, 064117.
(16) Lee, E.; Kim, S.; Jung, Y. Slowing Down of Ring Polymer Diffusion Caused by Inter-Ring Threading. *Macromol. Rapid Commun.* **2015**, *36*, 1115−1121.
(17) Michieletto, D.; Turner, M. S. A topologically driven glass in ring polymers. *Proc. Natl. Acad. Sci. U. S. A.* **2016**, *113*, 5195−5200.
(18) Michieletto, D. On the tree-like structure of rings in dense solutions. *Soft Matter* **2016**, *12*, 9485−9500.
(19) Ge, T.; Panyukov, S.; Rubinstein, M. Self-Similar Conformations and Dynamics in Entangled Melts and Solutions of Non-concatenated Ring Polymers. *Macromolecules* **2016**, *49*, 708−722.
(20) Michieletto, D.; Nahali, N.; Rosa, A. Glassiness and Heterogeneous Dynamics in Dense Solutions of Ring Polymers. *Phys. Rev. Lett.* **2017**, *119*, 197801.
(21) Kapnistos, M.; Lang, M.; Vlassopoulos, D.; Pyckhout-Hintzen, W.; Richter, D.; Cho, D.; Chang, T.; Rubinstein, M. Unexpected power-law stress relaxation of entangled ring polymers. *Nat. Mater.* **2008**, *7*, 997.
(22) Gooßen, S.; Brás, A. R.; Pyckhout-Hintzen, W.; Wischnewski, A.; Richter, D.; Rubinstein, M.; Roovers, J.; Lutz, P. J.; Jeong, Y.; Chang, T.; Vlassopoulos, D. Influence of the Solvent Quality on Ring Polymer Dimensions. *Macromolecules* **2015**, *48*, 1598−1605.
(23) Brás, A. R.; Pasquino, R.; Koukoulas, T.; Tsolou, G.; Holderer, O.; Radulescu, A.; Allgaier, J.; Mavrantzas, V. G.; Pyckhout-Hintzen, W.; Wischnewski, A.; Vlassopoulos, D.; Richter, D. Structure and dynamics of polymer rings by neutron scattering: breakdown of the Rouse model. *Soft Matter* **2011**, *7*, 11169−11176.
(24) Brás, A. R.; Gooßen, S.; Krutyeva, M.; Radulescu, A.; Farago, B.; Allgaier, J.; Pyckhout-Hintzen, W.; Wischnewski, A.; Richter, D. Compact structure and non-Gaussian dynamics of ring polymer melts. *Soft Matter* **2014**, *10*, 3649−3655.
(25) Gooßen, S.; Brás, A.; Krutyeva, M.; Sharp, M.; Falus, P.; Feoktystov, A.; Gasser, U.; Wischnewski, A.; Richter, D. Molecular Scale Dynamics of Large Ring Polymers. *Phys. Rev. Lett.* **2014**, *113*, 169302.
(26) Vlassopoulos, D. Macromolecular topology and rheology: beyond the tube model. *Rheol. Acta* **2016**, *55*, 613−632.
(27) Iwamoto, T.; Doi, Y.; Kinoshita, K.; Takano, A.; Takahashi, Y.; Kim, E.; Kim, T.-H.; Takata, S.-i.; Nagao, M.; Matsushita, Y.

DOI: 10.1021/acsmacrolett.8b00828
ACS Macro Lett. 2019, 8, 155−160

Conformations of Ring Polystyrenes in Semidilute Solutions and in Linear Polymer Matrices Studied by SANS. *Macromolecules* **2018**, *51*, 6836.
(28) De Gennes, P.-G. *Scaling Concepts in Polymer Physics*; Cornell University Press: Ithaca, 1979.
(29) Doi, M.; Edwards, S. F. *The Theory of Polymer Dynamics*; Oxford University Press: New York, 1986.
(30) Rubinstein, M.; Colby, R. H. *Polymer Physics*; Oxford University Press: New York, 2003.
(31) Rubinstein, M. Dynamics of ring polymers in the presence of fixed obstacles. *Phys. Rev. Lett.* **1986**, *57*, 3023−3026.
(32) Rosa, A.; Everaers, R. Conformational statistics of randomly-branching double-folded ring polymers. https://arxiv.org/abs/1808.06861 **2018**, 12 pages. *Eur. Phys. J. E*, accepted for publication.
(33) Smrek, J.; Grosberg, A. Y. Minimal Surfaces on Unconcatenated Polymer Rings in Melt. *ACS Macro Lett.* **2016**, *5*, 750−754.
(34) Tsalikis, D. G.; Mavrantzas, V. G. Threading of Ring Poly(ethylene oxide) Molecules by Linear Chains in the Melt. *ACS Macro Lett.* **2014**, *3*, 763−766.
(35) Tsalikis, D. G.; Mavrantzas, V. G.; Vlassopoulos, D. Analysis of Slow Modes in Ring Polymers: Threading of Rings Controls Long-Time Relaxation. *ACS Macro Lett.* **2016**, *5*, 755−760.
(36) Michieletto, D.; Marenduzzo, D.; Orlandini, E.; Turner, M. S. Ring Polymers: Threadings, Knot Electrophoresis and Topological Glasses. *Polymers* **2017**, *9*, 349.
(37) Rosa, A.; Everaers, R. Structure and dynamics of interphase chromosomes. *PLoS Comput. Biol.* **2008**, *4*, e1000153.
(38) Everaers, R.; Sukumaran, S. K.; Grest, G. S.; Svaneborg, C.; Sivasubramanian, A.; Kremer, K. Rheology and microscopic topology of entangled polymeric liquids. *Science* **2004**, *303*, 823−826.
(39) Uchida, N.; Grest, G. S.; Everaers, R. Viscoelasticity and primitive-path analysis of entangled polymer liquids: from F-actin to polyethilene. *J. Chem. Phys.* **2008**, *128*, 044902.
(40) Bray, A. Theory of phase-ordering kinetics. *Adv. Phys.* **1994**, *43*, 357−459.
(41) Lifshitz, I.; Slyozov, V. The kinetics of precipitation from supersaturated solid solutions. *J. Phys. Chem. Solids* **1961**, *19*, 35−50.
(42) Kawakatsu, T.; Munakata, T. Kink Dynamics in a One-Dimensional Conserved TDGL System. *Prog. Theor. Phys.* **1985**, *74*, 11−19.

DOI: 10.1021/acsmacrolett.8b00828
ACS Macro Lett. 2019, 8, 155−160